The International Journal of Advanced Manufacturing Technology (2023) 128:5547–5559
https://doi.org/10.1007/s00170-023-12232-0

ORIGINAL ARTICLE

Response behavior of grain evolution to forming conditions during hot ring rolling of as-cast 100Cr6 steel

Jiadong Deng[1,2,3] · Dongxing Zhai[1] · Jun Guo[4] · Dongsheng Qian[2,3,4] · Yanhua Zhang[3]

Received: 19 December 2022 / Accepted: 26 August 2023 / Published online: 9 September 2023

Abstract

As-cast ring rolling is a short-process new forming technology for ring parts with obvious technical superiority compared to conventional ring rolling. The microstructure improvement of as-cast ring during rolling process is the most concern for its industrial application, which has important dependence on forming conditions. In this study, an experimentally verified FE model for grain evolution prediction during hot ring rolling (HRR) of as-cast 100Cr6 alloy steel is explored; the response laws of grain size and distribution of rolled ring to rolling ratio, feeding rate, rotational speed, and initial rolling temperature during HRR process are discussed based on FE simulation. The main results show that the advantageous response of grain evolution will generate to improve the grain refinement and grain uniformization with the proper increases of rolling ratio and feeding rate and the appropriate decreases of rotational speed and initial rolling temperature. The remarkable response sensitivity of grain evolution will be beneficial to effectively adjust the grain refinement and grain uniformization with the preferred forming condition of lower initial rolling temperature. Finally, an optimization for forming conditions is performed according to above rules, and its effectiveness for grain improvement is simulatively and experimentally evaluated, which verified the reliability of obtained results.

Keywords Hot ring rolling · As-cast 100Cr6 steel · Grain · Forming condition · Response behavior

1 Introduction

Hot ring rolling (HRR) is an advanced metal working technology for manufacturing seamless rings. HRR has wide application in the industrial productions of various ring-type mechanical parts, such as bearing, flange rings, gear rings, and train wheels, due to its various significant advantages such as low energy and material consumption, good forming accuracy, and high efficiency [1–4].

✉ Dongsheng Qian
dengjd@whut.edu.cn

1 School of Automotive Engineering, Wuhan University of Technology, Wuhan 430070, China

2 Hubei Key Laboratory of Advanced Technology for Automotive Components, Wuhan University of Technology, Wuhan 430070, China

3 Hubei Provincial Key Laboratory of Green Materials for Light Industry, Hubei University of Technology, Wuhan 430068, China

4 School of Materials Science and Engineering, Wuhan University of Technology, Wuhan 430070, China

However, to realize the ring rolling process, a redundant manufacturing chain from material to ring blank is needed, as shown in Fig. 1a; the large consumptions of energy, materials, and time in this process obviously decrease the technical-economical effect of ring rolling production. Aimed at this problem, some experts proposed a new combined casting-hot ring rolling technology, which directly processes the ring blank by casting and can short the conventional manufacturing chain and reduce the manufacturing consumption of ring blank significantly, as shown in Fig. 1b. The invention of this new ring rolling technology gains many attentions rapidly because of its apparent technical-economical superiority in industrial production, especially in the mass production of bearing rings.

With the rapid development of advanced equipments in automobile, railway, energy, aviation, and astronavigation, the property requirements of rings continuously increase to meet the complicated and changeable working conditions. Under this environment, both of academic research and industrial production of HRR have mainly focused on the microstructure evolution in order to realize the maximum property improvement of rings in recent years. For

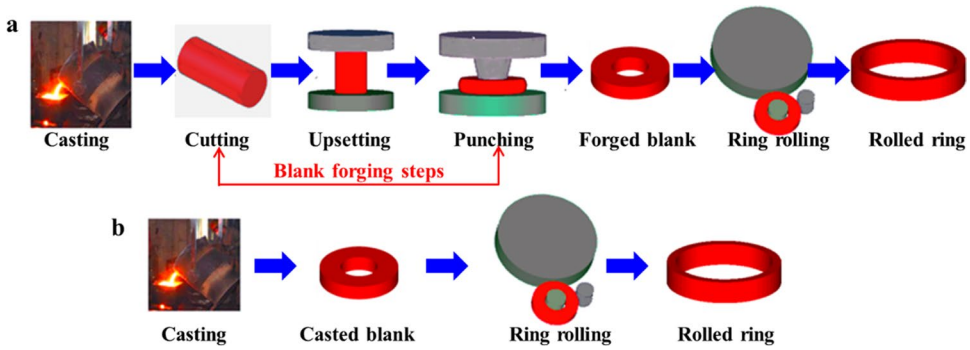

Fig. 1 **a** The conventional process chain of rings manufacturing with forged ring blank; **b** the new process chain of rings manufacturing with casted ring blank

conventional ring rolling process with forged ring blank, Qin et al. [5] studied the microstructure evolution in hot ring rolling of centrifugal casting Q235B steel; Chang et al. [6] did experimental research on some the hot ring rolling of centrifugally cast bimetallic rings. Sun et al. [7] revealed the effects of forming parameters on the grain evolution and recrystallization behavior of AISI 5140 alloy steel ring during hot rolling by FE simulation. Ryttberg and Wedel [8] investigated the microstructure and texture evolution in cold rolling of 100Cr6 ring experimentally. Wang et al. [9] modeled the microstructure evolution of titanium alloy during hot ring rolling using VUMAT subroutines. Qian and Pan [10] studied the distribution laws of grain sizes, dynamic recrystallization during blank forging, and ring rolling process. Tian et al. [11] studied the microscopic and macroscopic simulation of aluminum alloy rings by finite element simulation. Qi et al. [12] analyzed the effect of blooming temperature on radial-axial rolling forming of ring.

For ring rolling process with as-cast blank which is a new technology to manufacture rings, currently, the main research work is focused on reveling and controlling of microstructure evolution behavior, which is in favor of eliminating the cast defects. Guo et al. [13] proposed a multi-scale FE model of ring rolling process based on 42CrMo ingot blank and investigated the influence rules and mechanism of the rolling ratio on the recrystallized microstructure. Li et al. [14] studied the effects of initial rolling temperature on plastic deformation and dynamic recrystallization during hot ring rolling of as-cast 42CrMo ring blank based on DEFORM-3D. Li et al. [15] proposed using casting ring blank to form 42CrMo bearing ring and studied the microstructure evolution by FE simulation and experiment. Guo et al. [16] put forward a new approach coupling with both macroscopic and microscopic based on finite element theory and cellular automata model to reveal the deformation and microstructure evolution laws during casting-rolling compound forming process of as-cast 42CrMo alloy ring.

Above researches indicate that the microstructure evolution during HRR process has close dependence on the forming conditions like feeding amount, feeding speed, and temperature, which can provide important instruction for the microstructure improving by technological optimization. Nevertheless, as a widely used material for rings, especially for bearing rings, the microstructure evolution of as-cast 100Cr6 in HRR process regrettably gets few attentions and its correlations with the forming conditions are unclear, which obviously restricts the application of combined casting-hot ring rolling technology in bearing manufacturing. Therefore, in this study, using FEA and experiment, the accurate prediction of grain evolution during HRR of as-cast 100Cr6 steel is expectedly realized; the dependence between the grain evolution and the key forming conditions are expectedly revealed, and its instruction role for the grain improvement by optimizing of forming conditions is experimentally verified.

2 FE modeling for the HRR of as-cast 100Cr6

2.1 Microstructure evolution model of 100Cr6

Through hot compression experiments and mathematical modeling, the predicting models for the flow stress, austenite grain growth, and recrystallization behaviors of as-cast GCr15 (Chinese mark of 100Cr6) were developed as follows [17–19]:

(a) Flow stress

$$\dot{\varepsilon} = 3.326e12[\sinh(0.00824\sigma)]^{-4.80311}\exp(-306005/RT) \quad (1)$$

where $\dot{\varepsilon}$ is the stain rate; R is the universal gas constant (8.31 $J{\cdot}mol^{-1}{\cdot}K^{-1}$); T is the absolute temperature (K); Q is the activation energy of hot deformation ($KJ{\cdot}mol^{-1}$); σ is the true stress (MPa).

(b) Austenite grain growth

$$d_g = \sqrt[4.133]{d_0^{4.133} + 6.685\times10^{31}t\exp\left(-6.8\times10^5/RT\right)} \quad (2)$$

where d_g is the average austenite grain size at holding time of t (μm); d_0 is the initial average austenite grain size; t is the holding time (s).

(c) Dynamic recrystallization (DRX)

$$\varepsilon_c = 0.78\varepsilon_p \tag{3}$$

$$\varepsilon_p = 0.0338 d_0^{0.0342} \dot{\varepsilon}^{0.1968} \exp\left(23550/RT\right) \tag{4}$$

$$\varepsilon_{0.5} = 0.0087 d_0^{0.0841} \dot{\varepsilon}^{0.1733} \exp\left(35484/RT\right) \tag{5}$$

$$X_{drex} = 1 - \exp\left[-2.67\left(\frac{\varepsilon - \varepsilon_c}{\varepsilon_{0.5}}\right)^{1.036}\right] \tag{6}$$

$$d_{drex} = 7.751 d_0^{0.410} \varepsilon^{-0.586} \dot{\varepsilon}^{-0.0057} \exp\left(-8834.6/RT\right) \tag{7}$$

where ε_c is the critical strain; ε_p is the peaking strain; $\varepsilon_{0.5}$ is the strain of 50% dynamic recrystallization; X_{drex} is the dynamic recrystallization fraction; d_{drex} is the grain size of DRX (μm); ε is the strain.

(d) Static recrystallization (SRX)

$$t_{0.5} = 2.04 \times 10^{-13} d_0^{0.01} \varepsilon^{-3.29} \dot{\varepsilon}^{-1.07} \exp\left[225860/(RT)\right] \tag{8}$$

$$X_{srex} = 1 - \exp\left[-0.693\left(t/t_{0.5}\right)^{0.35}\right] \tag{9}$$

$$d_{srex} = 6380 d_0^{0.32} \varepsilon^{-0.3} \dot{\varepsilon}^{-0.04} \exp\left(-23763/RT\right) \tag{10}$$

where X_{srex} is the static recrystallization fraction; $t_{0.5}$ is the time for the recrystallizing volumetric fraction of 50% (s); d_{srex} is the grain size of SRX (μm).

(e) Average grain size

$$d_a = X_{drex} \times d_{drex} + X_{srex} \times d_{srex} + \left(1 - X_{drex} - X_{srex}\right) \times d_0 \tag{11}$$

Above-mentioned models had been proved that can accurately describe the microstructure evolution behaviors of as-cast 100Cr6 during hot deformation process, and they were employed for FE modeling process.

2.2 FE modeling

Hot ring rolling is a rolling process of hot processing. In the hot rolling process, the drive roll is active roll which is driven and rotated by the main motor of the ring rolling mill through the reducer, guide roller, and mandrel are follower rolls that can rotate freely, the initial temperature of the ring is heated to 1150 °C.

Based on material models, a subroutine of microstructure evolution model of as-cast 100Cr6 is developed using FORTRAN language under SIMUFACT environment, and it was embed into the coupled thermo-mechanical FE model of HRR (Fig. 2) to realize the microstructure evolution analysis during the simulation process according to the calculated field variables of macrodeformation. The flow chat of microstructure evolution modeling in subroutine is shown in Fig. 3.

The thermophysical properties of material are given by the soft. The average grain size of ring blank in FE model is 60 μm, which was set by measuring and evaluating the actual as-cast 100Cr6 ring blank. The main parameters of the FE model considering the HRR experimental verification are given in Table 1.

In Table 1, the rolling ratio K is defined as [20]:

$$K = A_0/A \tag{12}$$

where A_0 and A are the cross-section areas of the ring blank and the rolled ring, respectively. In this paper, the rolling ratio K can be defined as the ratio of the thickness of ring blank H_0 to the thickness of rolled ring H without considering the height change of the rolled ring.

The key techniques for FE modeling can be described as follows:

(1) The rolls are considered as isothermal analytical rigid bodies and their deformation and temperature variations are ignored to diminish computational calculation time. The workpiece is defined as a deformable body.
(2) The hexahedron element with eight nodes is adopted to discrete the workpiece. In addition, the adaptive remeshing technique is also employed to deal with the problem of element distortion.
(3) The axial metal flow of the end surfaces of workpiece is constrained to symbolize the close rolling pass effects on the ring in actual HRR experiment.

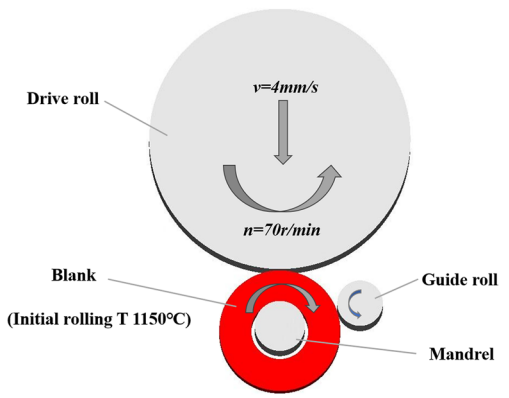

Fig. 2 3-D coupled thermo-mechanical FE model of HRR

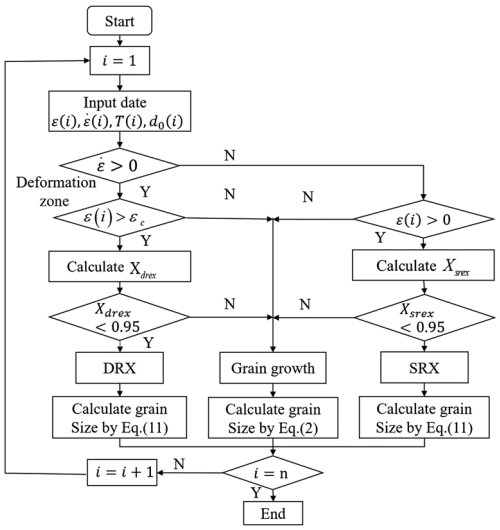

Fig. 3 Flow chart of microstructure modeling steps during ring rolling

Table 1 Main parameters of FE model

Parameters	Values
Out diameter of ring blank/mm	265
Inner diameter of ring blank/mm	125
Height of ring blank/mm	40
Diameter of driver roll/mm	585
Diameter of guide roll/mm	100
Diameter of mandrel/mm	110
Rotation speed of driver roll/r·min^{-1}	70
Feed speed of driver roll/mm·s^{-1}	4
Total radial thickness reduction/mm	20
Initial rolling temperature/°C	1150
Rolls temperature/°C	80
Friction coefficient	0.3

(4) Three contact pairs are defined between the driver roll and the workpiece, the mandrel and the workpiece, and the guide roll and the workpiece, respectively. Heat generation and heat transmission are set at the interface of each contact pair; heat radiation is considered between the workpiece and the ambient environment. Coulomb friction is adopted between each contact pair.

2.3 Experimental verification

To testify the reliability of the FE model, HRR experiment of as-cast 100Cr6 was carried out on D51-350 NC HRR mill, and the related experimental parameters are same with the FE model shown in Table 1. As shown in Fig. 4, three rolled rings with different deformation amount were obtained by HRR experiment. The radial feeding degree is defined as the ratio of the feeding amount ΔH to total radial thickness reduction ΔH_{total}.

The comparison of temperature of the rolled rings between experiment and simulation is shown as Fig. 5, and the maximum relative error between the actual temperature of the thermometer and the simulation temperature is within 5%, which indicates that the model is reliable.

The comparison of average grain size of the rolled rings between experiment and simulation was performed, as shown in Fig. 6, and Fig. 7 shows the experimental results of grain size distribution in inner layer under different deformation amount. Here, considering the nonuniform grain distribution, two points located at the outer layer and inner layer of the rolled rings are selected respectively for comparison; the experimental values of grain sizes were observed by Zeiss metallographic microscope and measured using linear intercept method; the simulated grain sizes were calculated by the FE model in Section 2.2. Figure 6 indicates that the simulated values of grain size are in good agreements with the experimental ones; thus, the FE model is testified valid and reliable to predict the grain evolution during the HRR process of as-cast 100Cr6.

Fig. 4 HRR experiment of as-cast 100Cr6: **a** D51-350 NC HRR mill; **b** HRR process; **c** rolled rings under different deformation amount

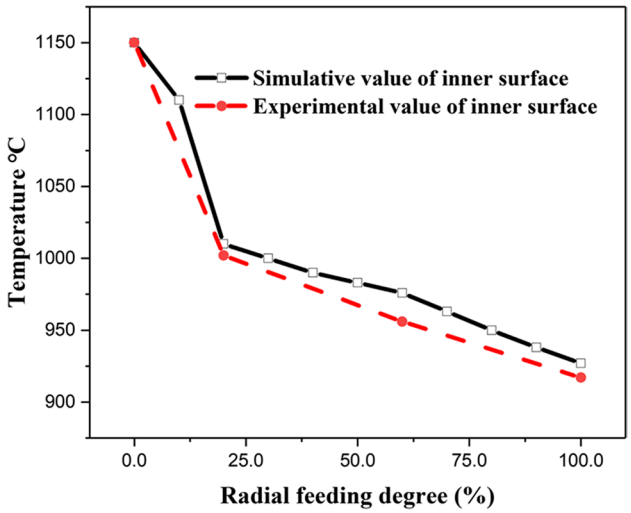

Fig. 5 Comparison of temperature of the rolled rings between experiment and simulation

3 Results and discussions

Employing the developed FE model, the prediction of grain evolution behavior during HRR of as-cast 100Cr6 can be realized. In HRR process, rolling ratio K, feeding rate v, rotational speed n, and initial rolling temperature T are the four key process parameters directly affected the field variables of strain, stain rate, and temperature, which are regarded as the critical factors for the grain evolution. So, in this paper, the HRR processes with different values of the four process parameters are simulated so as to investigate the response behaviors of the grain evolution to the forming conditions.

3.1 Simulation conditions

Four groups of forming conditions are considered in HRR simulations.

Case 1: $K = \{1.1, 1.5, 1.7, 1.8, 2.0\}$, $v = 4.0$ mm/s, $n = 70$ r/min, $T = 1150$ °C
Case 2: $v = \{1.0, 2.0, 3.0, 4.0\}$ mm/s, $K = 1.5$, $n = 70$ r/min, $T = 1150$ °C
Case 3: $n = \{50, 60, 70, 80\}$ r/min, $K = 1.5$, $v = 4.0$ mm/s, $T = 1150$ °C
Case 4: $T = \{950$ °C, 1050 °C, 1150 °C, 1250 °C$\}$, $K = 1.5$, $v = 4.0$ mm/s, $n = 70$ r/min

3.2 Evaluated indices for discussion

It is obvious that the grain size and grain distribution have close relevance with the material property, and the fine and uniform grains usually means the good mechanical property, which are expectedly obtained by forming process. Hence, two parameters are adopted to describe the grain evolution during the HRR process. One parameter is refinement degree of grain RDG; it is defined as:

$$RDG = \frac{d_0 - d_{avg}}{d_0} \times 100\% \tag{13}$$

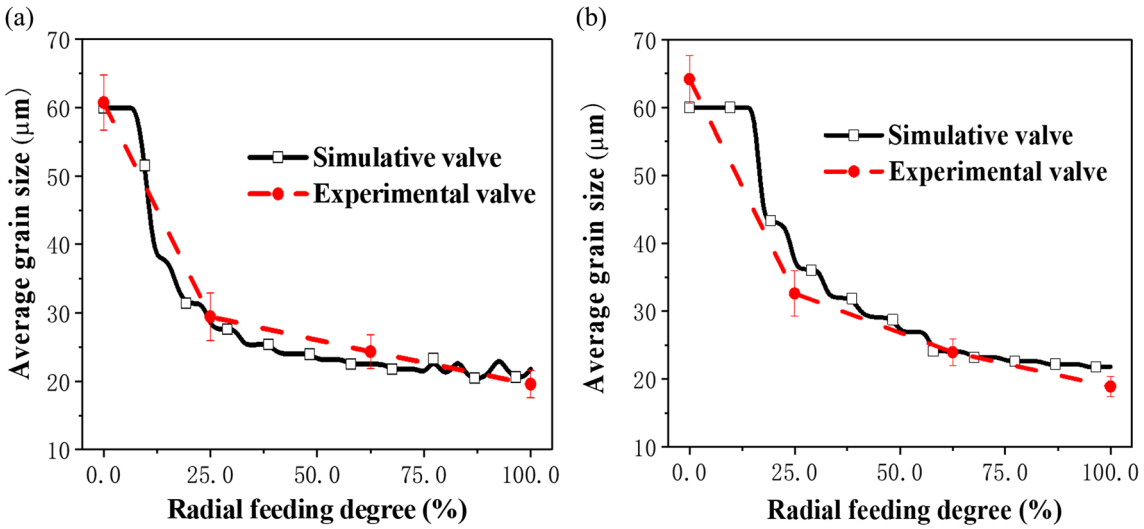

Fig. 6 Comparison of average grain size of the rolled rings between experiment and simulation: **a** outer layer; **b** inner layer

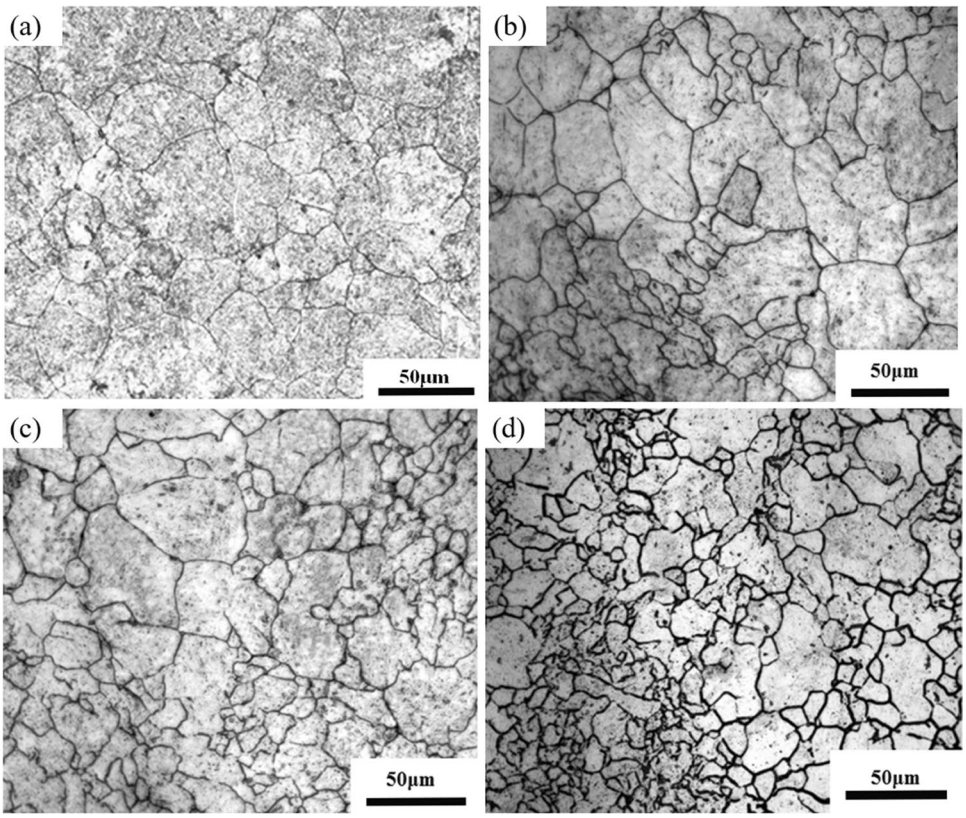

Fig. 7 Experimental results of grain size distribution in inner layer during rolling process: **a** 0%; **b** 25%; **c** 63%; **d** 100%

$$d_{avg} = \frac{1}{n}\sum_{i=1}^{n} d_i \tag{14}$$

where n is the node number of the rolled ring, d_i is the average grain size of node i, and d_{avg} is the average grain size of the rolled ring.

Another parameter is the inhomogeneity of grain *IHG*; it is defined as:

$$IHG = \sqrt{\sum_{i=1}^{n} \left(d_i - d_{avg}\right)^2 / n} \tag{15}$$

RDG and *IHG* represent the evolution of grain size and grain distribution during HRR process, the more value of *RDG*, the smaller the grain; the less value of *IHG*, the more uniform the grain distribution.

3.3 Response rules of grain evolution to forming conditions

3.3.1 Rolling ratio

In simulation case 1, the response of *RDG* and *IHG* to rolling ratio *K* is revealed, as shown in Figs. 8 and 9.

Figure 8 shows that obvious grain refinement in the whole ring regions can be observed with the increase of rolling ratio, and the grain response in the outer and inner layers of ring is stronger than that in the middle layer of ring. Figure 9 illustrates that with *K* increases, the advantageous response of grain size generates embodied as the *RDG* increasing, while the advantageous and adverse responses of grain distribution generate successively, which is represented by the *IHG* increasing in first and decreasing at last.

As rolling ratio *K* increases, the plastic deformation degree also increases; thus, the larger strain level promotes the recrystallization of material and results in more recrystallized grains with small size. But the nonuniform deformation in HRR process leads to the high stain and low temperature at surface layers [14], which causes well grain refinement of the surface layers. So, with the increase of *K*, the integrated grain refinement of rolled ring makes grain distribute uniformly at first, then the difference of grain refinement degree between the surface layers and middle layer goes against the uniformization of grain distribution. Hence, in HRR process of as-cast 100Cr6 steel, proper increasing rolling ratio can induce the advantageous response of grain evolution and improve the grain size and distribution.

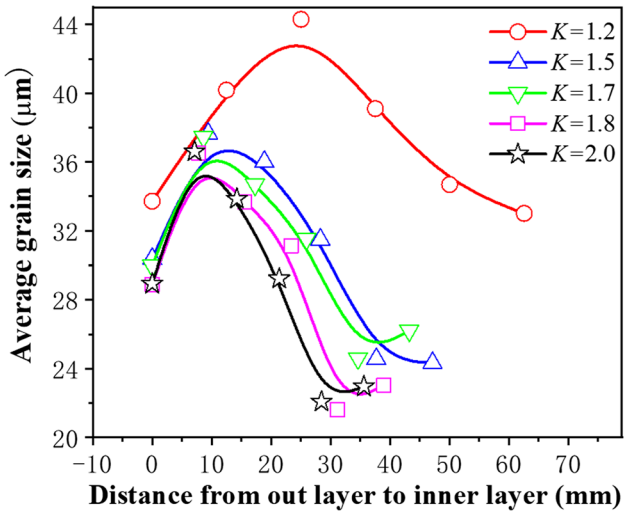

Fig. 8 Relationship between radial distribution of grain size and rolling ratio *K*

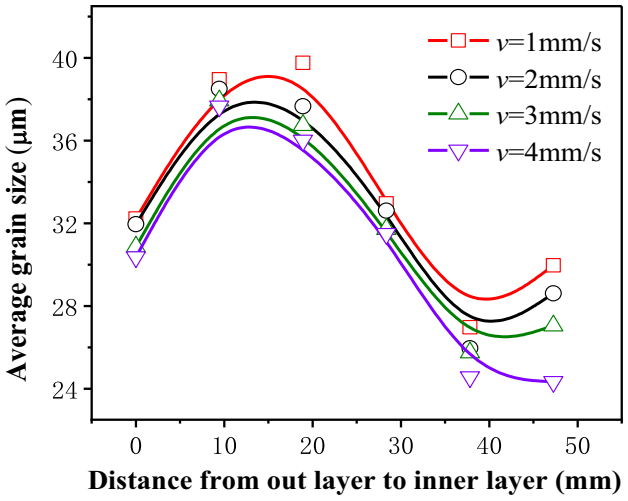

Fig. 10 Relationship between radial distribution of grain size and feeding rate *v*

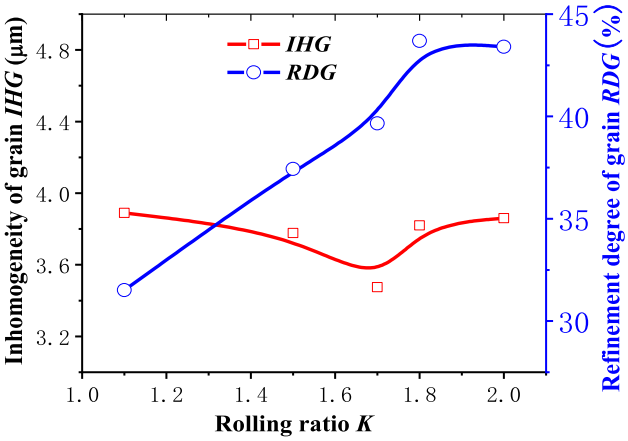

Fig. 9 Responses of *RDG* and *IHG* to rolling ratio *K*

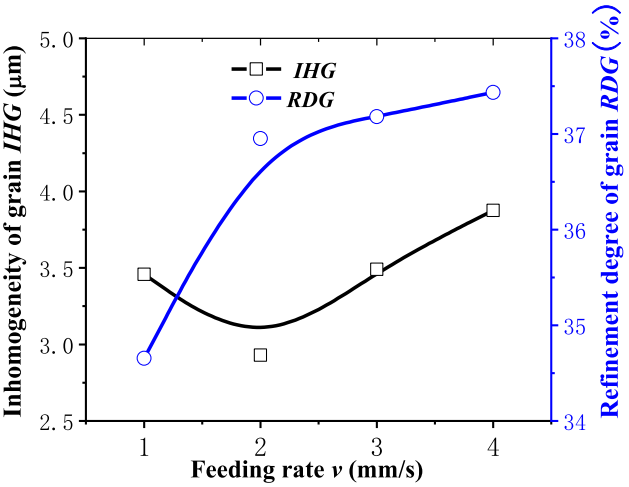

Fig. 11 Responses of *RDG* and *IHG* to feeding rate *v*

3.4 Feeding rate

In simulation case 2, the response of *RDG* and *IHG* to feeding rate *v* is determined, as shown in Figs. 10 and 11.

In Fig. 10, we can see that when feeding rate *v* increases, grain refinement presents at different ring locations and the grain refinement degree of outer and inner layers is larger than middle layer. Figure 11 provides that with *v* increases, grain size has the advantageous response expressed by the increase of *RDG*, while the V-shaped curve of *IHG* demonstrates that grain distribution produces the advantageous and adverse responses successively.

The larger the feeding rate *v*, the higher the stain rate of material is, which is beneficial for the formation of small recrystallized grains. Furthermore, as *v* becomes larger, the feed amount per revolution increases, the plastic zone extends to the middle layer more easily, and plastic deformation becomes more homogeneous [21], which is beneficial to the uniformity of grain distribution. However, with the sustained increase of *v*, the difference of deformation level between the surface layers and middle layer becomes larger, and this leads to the increased difference of grain refinement level between them, as shown in Fig. 10, which advances in the increase of IHG. Therefore, in HRR process of as-cast 100Cr6 steel, reasonable feed rate should be designed to obtain the advantageous response of grain evolution.

3.4.1 Rotational speed

In simulation case 2, the response of *RDG* and *IHG* to rotational speed *n* is obtained, as shown in Figs. 12 and 13.

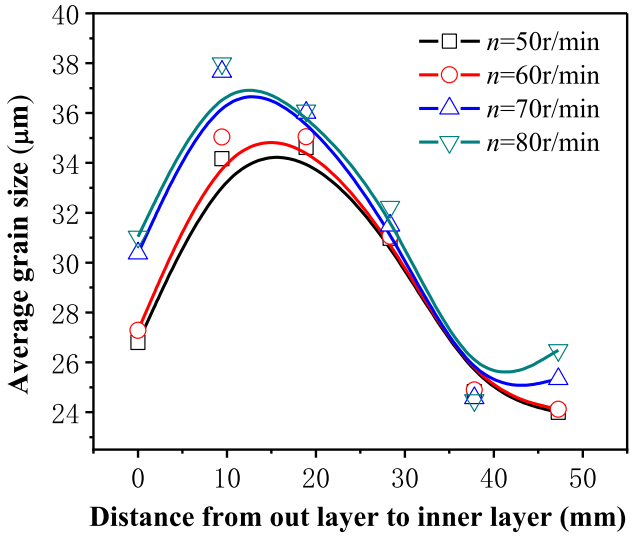

Fig. 12 Relationship between radial distribution of grain size and rotational speed *n*

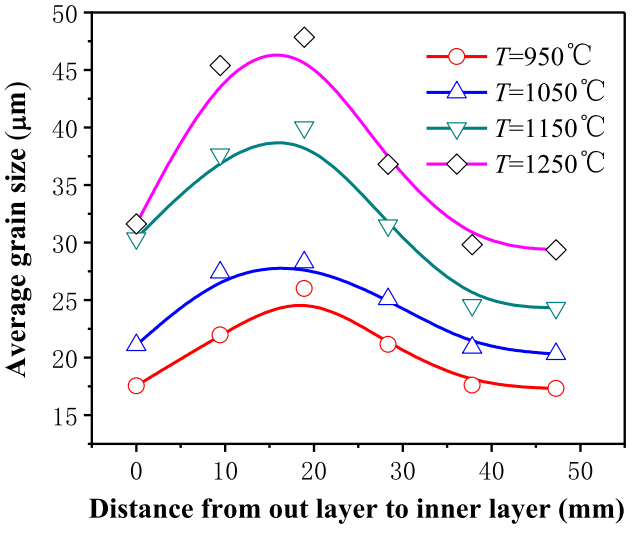

Fig. 14 Relationship between radial distribution of grain size and initial rolling temperature *T*

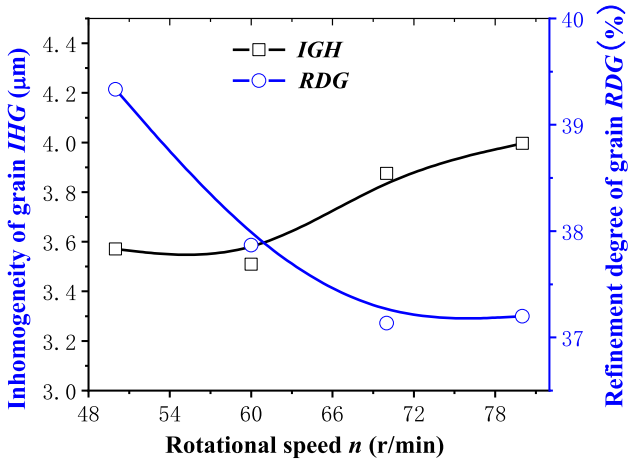

Fig. 13 Responses of *RDG* and *IHG* to rotational speed *n*

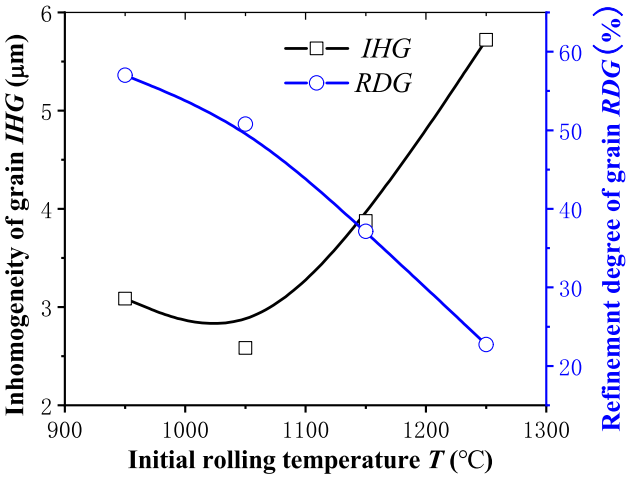

Fig. 15 Responses of *RDG* and *IHG* to initial rolling temperature *T*

From Fig. 12, it can be seen that with the increase of rotational speed *n*, apparent grain coarsening produces at the outer and inner layers of ring, while the grain size of middle layer has slight increase. Figure 13 indicates that with *n* increases, adverse responses of grain size and grain distribution both produce because of the *RDG* decreases and *IHG* increases.

From the reference [20], we know that the feed amount per revolution decreases with increased rotational speed; thus, the deformation degree reduces and the penetrability of plastic zone weakens; these restrict the grain refinement and uniform distribution, especially for the surface layers because the responses of surface layers to the forming conditions are more sensitive than the middle layer in HRR process, which can be concluded from reference [21]. So, in HRR process of as-cast 100Cr6 steel, the smaller rotational speed should be employed within the scope of stable rolling conditions [20] for the advantageous response of grain evolution.

3.4.2 Initial rolling temperature *T*

In simulation case 3, the response of *RDG* and *IHG* to initial rolling temperature *T* is presented, as shown in Figs. 14 and 15.

Figure 14 provides that obvious grain coarsening occurs in the whole ring regions with the increase of initial rolling temperature *T*, particularly in the middle layer. Figure 15 shows

that with T increases, the adverse response of grain refinement exists reflected by the decreased *RDG*, and a changed response from advantageous to adverse is created by grain distribution expressed by the V-shaped *IHG* curve. This is basically consistent with findings of Qi et al. [12].

Although larger T is beneficial for the recrystallization of material, it also means that the recrystallized grains have better condition to grow. When the forming conditions can sufficiently ensure the fully recrystallization to produce in HRR process, the contribution of larger T to the growing of recrystallized grains is significant, thus decrease the grain refinement degree in summary, and its influence on the middle layer is more obvious because the grains in the middle layer always gains less refinement level than the surface layers under the same forming conditions. Furthermore, the lower temperature restricts the sufficient and uniform recrystallization to generate in the different ring regions, thus harmful to the homogeneous grain distribution, and the higher temperature causes to the more obvious temperature gradient along the ring thickness during the deformation process thus also disadvantageous to the uniform grain distribution. Accordingly, the initial rolling temperature should be selected suitably to get the advantageous response of grain distribution and possibly limit the adverse response of grain size.

3.5 Response sensitivity of grain evolution to forming conditions

In the above analysis, the response rule of grain evolution to each forming condition was revealed, respectively. To compare the response behavior of grain evolution to different forming conditions, a further study was carried out in this section.

Firstly, as the measuring units of the four forming conditions are different, it is necessary to make a unity of them. The normalization method was adopted to make them uniform according to Eq. (16). Then, the refinement degree of grain *RDG* and inhomogeneity of grain *IHG* can be compared respectively in one horizontal coordinate axis to different forming conditions, as shown in Figs. 16 and 17.

$$f_{(X)} = \frac{X - X_{\min}}{X_{\max} - X_{\min}} \tag{16}$$

where $f_{(X)}$ is the value after normalization of different forming conditions and its value is from 0 to 1, X is the value of different forming conditions, $X_{\min}$ is the minimum value of X, and $X_{\max}$ is the maximum value of X.

Figure 16 shows that initial rolling temperature T has a more remarkable response of *RDG* than other three forming conditions. In the adjustment range of each forming condition, changing rolling temperature T individually can obtain the maximum refinement degree of grain *RDG*, changing rolling ratio K is next, and changing feeding rate v can hardly increase *RDG*. Figure 17 indicates that initial rolling temperature T also has a more obvious response of *IHG* than other three forming conditions. In the adjustment range of each forming condition, changing rolling temperature T individually can obtain the minimum inhomogeneity of grain *IHG*, changing feeding rate v is next, and changing rolling ratio K and rotational speed n can obtain the similar inhomogeneity of grain *IHG*.

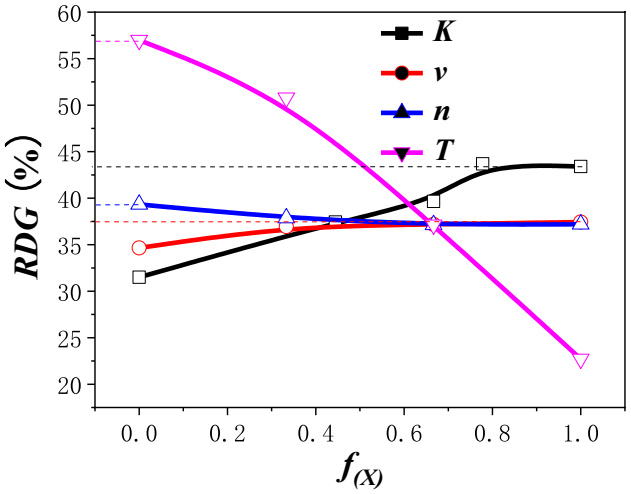

Fig. 16 Responses of *RDG* to different forming conditions

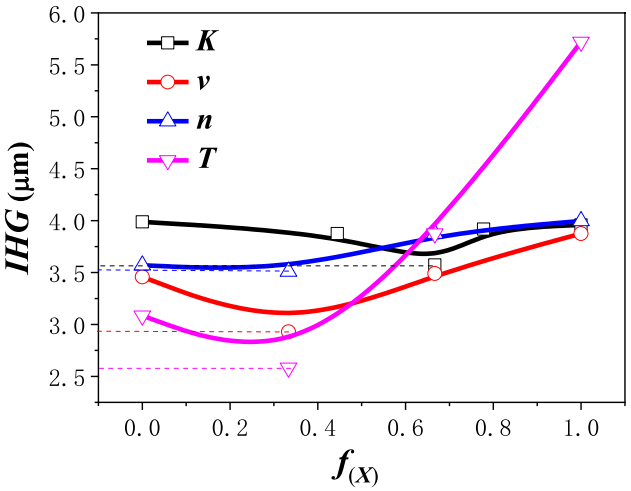

Fig. 17 Responses of *IHG* to different forming conditions

To make a further study on the response behavior of grain evolution to forming conditions. The response sensitivity is proposed to measure the response size and speed of grain evolution to forming conditions. Thus, the maximum response amplitude of *IHG* and *RDG* to different forming conditions can be selected to characterize the response size of grain evolution. The response rate of *IHG and RDG* with $f_{(X)}$ may reflect the response speed of grain evolution to forming conditions.

The maximum response amplitude of *RDG* to different forming conditions MRA_{RDG} can be expressed as:

$$MRA_{RDG} = RDG_{\max} - RDG_{\min} \tag{17}$$

where $RDG_{\max}$ is the maximum value of *RDG* in the adjustment range of each forming condition, and $RDG_{\min}$ is the minimum value of *RDG*.

The maximum response amplitude of *IHG* to different forming conditions MRA_{IHG} can be also defined as:

$$MRA_{IHG} = IHG_{\max} - IHG_{\min} \tag{18}$$

where $IHG_{\max}$ is the maximum value of *IHG* in the adjustment range of each forming condition, and $IHG_{\min}$ is the minimum value of *IHG*.

MRA_{RDG} and MRA_{IHG} respectively represent response size of grain size and grain inhomogeneity to forming condition. The more value of MRA_{RDG}, the larger degree the grain size can be adjusted when changing one forming condition. The more value of MRA_{IHG}, the larger degree the grain inhomogeneity can be adjusted when changing one forming condition.

Figure 18 shows the maximum response amplitudes of *RDG* and *IHG* to different forming conditions. It indicates that the response sizes of *RDG* and *IHG* to initial rolling temperature *T* are both the maximum of the four forming conditions. Rolling ratio *K* ranks the second for the response size of *RDG*; feeding speed *v* and rotational speed *n* have a similar response size of *RDG*. For the response size of *IHG*, feeding speed *v* is the next; rolling ratio *K* and rotational speed *n* keep in a similar level. That is to say, to adjust the refinement degree of grain or inhomogeneity of grain of the rolled ring, the initial rolling temperature can make the maximum changing degree. This result is agreed with the study in reference [22].

The response rate of *RDG* and *IHG* with $f_{(X)}$ can be calculated by the following expressions:

$$RRX_{RDG} = \frac{\Delta RDG}{\Delta f_{(X)}} \tag{19}$$

$$RRX_{IHG} = \frac{\Delta IHG}{\Delta f_{(X)}} \tag{20}$$

where RRX_{RDG} is the response rate of *RDG*, RRX_{IHG} is the response rate of *IHG*, and ΔRDG is the variation of *RDG* when $f_{(X)}$ changes with $\Delta f_{(X)}$. ΔIHG is the variation of *IHG* when $f_{(X)}$ changes with $\Delta f_{(X)}$.

RRX_{RDG} and RRX_{IHG} respectively represent response speed of grain size and grain inhomogeneity to forming condition. The more value of RRX_{RDG}, the faster variation the grain size can be realized when adjusting one forming condition. The more value of RRX_{IHG}, the faster variation the grain inhomogeneity can be realized when adjusting one forming condition.

Figure 19 provides that the response rate of *RDG* to the initial rolling temperature *T* is negative and its absolute value is the largest. That is to say, to decrease *T* is the most obvious way to increase *RDG*. The response rate of *RDG* to rolling ratio *K* is positive and the value is in the second level. Besides when $f_{(X)}$ increases to a certain value, the response rate will decrease quickly closing to 0. It means that to increase *K* is the second preferred way to increase *RDG*, but when *K* increases to a certain value, the *RDG* increases hardly. The response rates of *RDG* to feeding speed *v* and rotational speed *n* are in similar level, but the former one is negative and the latter one is positive. Thus, to decrease *v* will reduce *RDG* and to decrease *n* may increase *RDG*.

Figure 20 indicates that the response rate of *IHG* to the initial rolling temperature *T* is changing from negative value to positive value and its absolute value is the largest. That is to say, to decrease *T* is the fastest way to decrease *IHG*. And when *T* is selected between 950 and 1050 °C, *IHG* is in a lower level. Feeding speed *v* is the second factor to affect the response rate of *IHG*. When *v* is close to 2

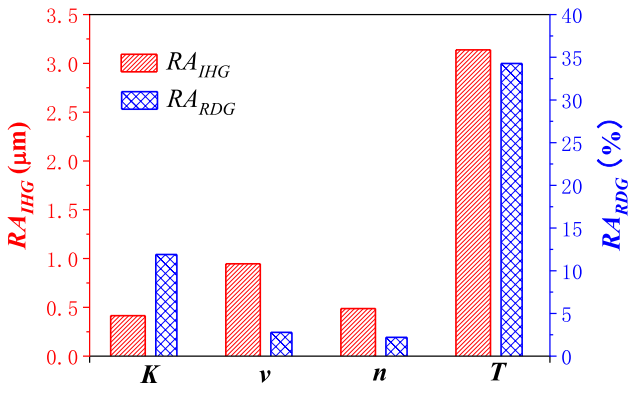

Fig. 18 Maximum response amplitudes of *IHG* and *RDG* to different forming conditions

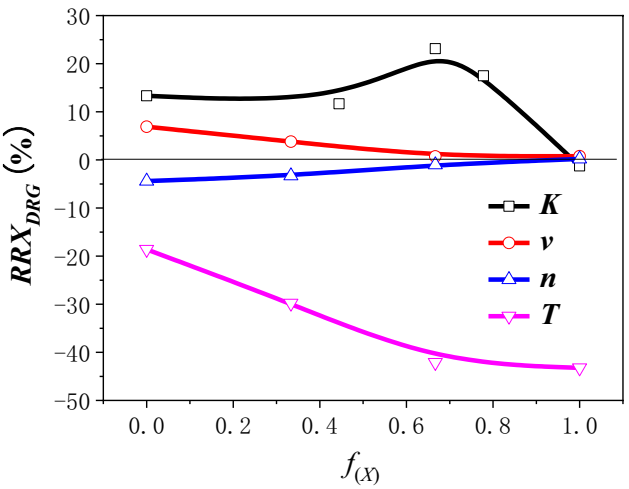

Fig. 19 Response rates of *RDG* to different forming conditions

mm/s, IHG locates in a valley value. Rolling ratio *K* ranks the third. When *K* is selected between 1.5 and 1.7, a small value of *IHG* will occur. Rotational speed *n* has a weak effect on the response rate of *IHG*. When *n* is selected in a small level, a well *IHG* can be obtained.

4 Results verification

It is obvious that the response of grain evolution to forming conditions has important relation with the forming condition optimization to improve microstructure of the rolled ring. According to the grain evolution response investigated above, the optimization for the initial forming conditions in Table 1 can be performed, as shown following:

(a) Initial forming conditions: $k = 1.5$, $T = 1150$ °C, $v = 4$ mm/s, $n = 70$ r/min

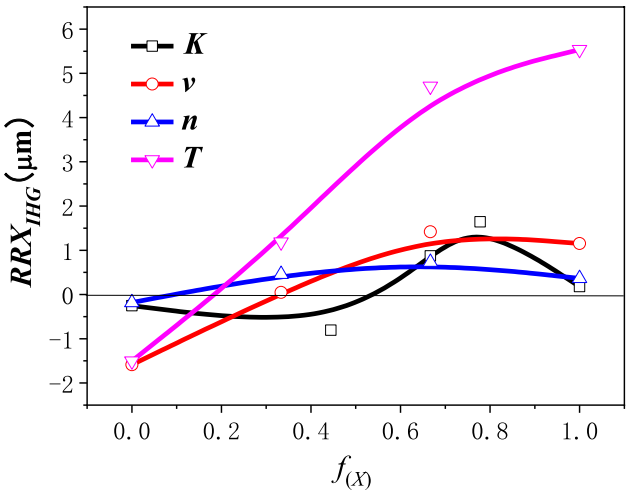

Fig. 20 Response rates of *IHG* to different forming conditions

(b) Optimized forming conditions: $k = 1.8$, $T = 950$ °C, $v = 4$ mm/s, $n = 50$ r/min

Then, simulation and experiment of HRR with as-cast 100Cr6 steel were carried out with above two groups of forming conditions to evaluate the effect of forming condition optimization on grain improvement and verify the reliability of obtained results.

From the simulation results as shown in Fig. 21, it can be seen that under the optimized forming conditions, the grain size of whole ring decreases, and the difference of grain sizes between the surface layers and middle layer reduces. The comparisons in Fig. 22 indicate that the grain size and grain distribution of the rolled ring improve significantly with the optimized forming conditions.

Figures 23 and 24 show the experimental grain comparisons under the initial and optimized forming conditions. The average grain sizes of the middle layer and inner layer under the initial forming conditions were respectively 41 μm and 25 μm. Under optimized forming conditions, the average grain sizes of the middle layer and inner layer under the initial forming conditions were respectively improved to 23 μm and 15 μm. As it can be seen that the grain size was decreased significantly and the difference of grain sizes between the inner layers and middle layer was reduced with the optimized forming conditions. It has a good agreement with the simulative result.

5 Conclusions

In our work, the response behavior of grain evolution to forming conditions during hot ring rolling of as-cast 100Cr6 steel has been studied, including rolling ratio, feeding rate, rotational speed, and initial rolling temperature. Based on the analysis, an optimization for forming conditions is performed by simulation and experiment successfully. The research can provide a scientific guidance for optimizing parameters of the

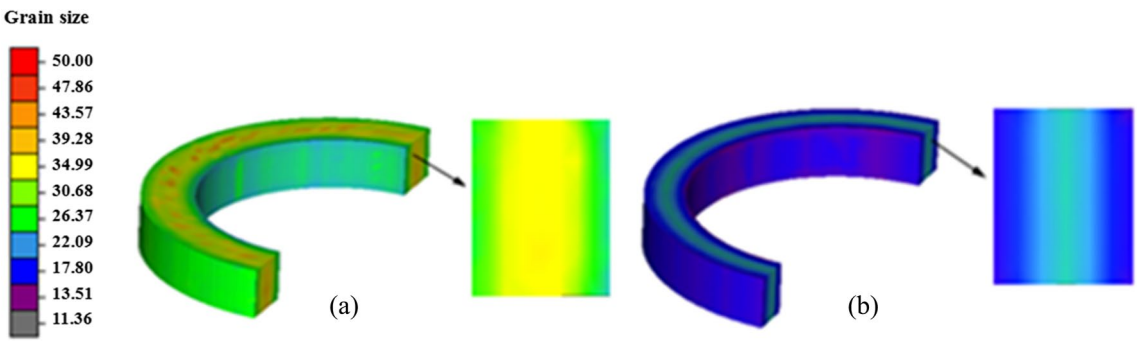

Fig. 21 Grain chats of the rolled rings under the initial and optimized forming conditions: **a** initial forming conditions; **b** optimized forming conditions

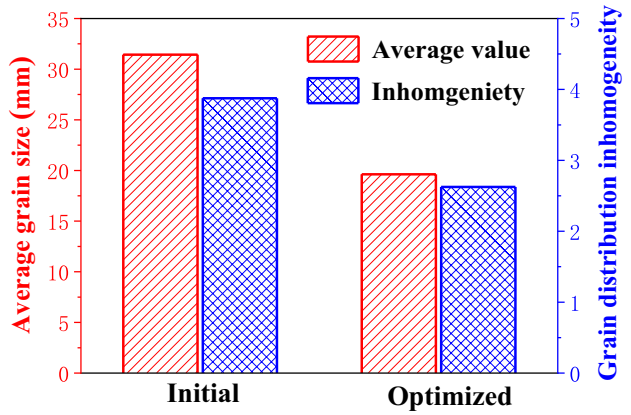

Fig. 22 Simulative comparisons of grain size and grain distribution between the rolled rings with initial forming conditions and optimized forming conditions

forming condition, which is beneficial to the development and application of the new combined casting-ring rolling technology. The main conclusions can be drawn as follows:

(1) When rolling ratio or feeding rate increases, the refinement degree of grain increases, and the inhomogeneity of grain firstly decreases then increases. When rotational speed increases, the refinement degree of grain decreases, and the inhomogeneity of grain increases. When initial rolling temperature increases, the refinement degree of grain decreases, and the inhomogeneity of grain firstly decreases then increases. The advantageous response of grain evolution will generate to improve the grain refinement and grain uniformization with the proper increases of rolling ratio and feeding rate and the appropriate decreases of rotational speed and initial rolling temperature.

(2) For the refinement degree of grain, initial rolling temperature has the most remarkable response sensitivity, rolling ratio is the next, and then rotational speed and feeding rate have similar response sensitivity. For the inhomogeneity of grain, initial rolling temperature also shows the most remarkable response sensitivity, feeding rate ranks the second, and then rolling ratio and rotational speed lie in similar level. The remarkable response sensitivity of grain evolution will be beneficial to effectively adjust the grain refinement and grain uniformization with the preferred forming condition of lower initial rolling temperature.

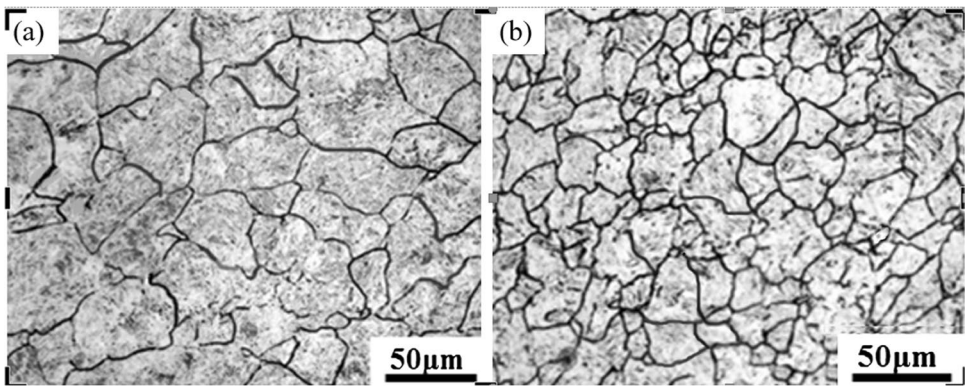

Fig. 23 Experimental grain sizes of the rolled rings under the initial forming conditions: **a** middle layer; **b** inner layer

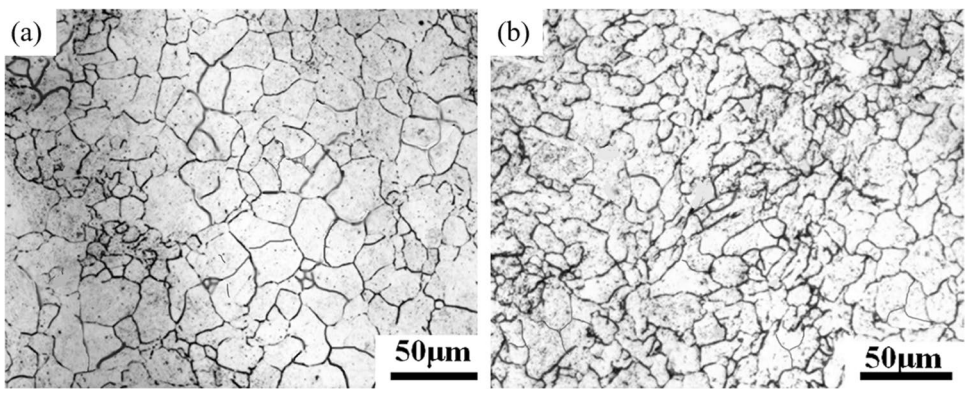

Fig. 24 Experimental grain sizes of the rolled rings under the optimized forming conditions: **a** middle layer; **b** inner layer

Author contributions Conceptualization (DJD, QDS, ZDX), methodology (DJD, QDS, ZDX), software (DJD), validation (DJD, ZDX), formal analysis (ZDX), investigation (GJ, DJD), resources (DJD, QDS), data curation (QDS, DJD), writing—original draft (DJD, ZDX), writing—review and editing (ZDX), visualization (GJ, ZDX), supervision (QDS, DJD, ZYH), project administration (DJD, ZYH), funding acquisition (QDS, DJD).

Funding This work was supported by National Key Research and Development Project (2018YFA0702905), the 111 Project (B17034), the Innovative Research Team Development Program of Ministry of Education of China (No. IRT_17R83), and Hubei Key Research and Development Project (2021BAA019).

Data availability The datasets used or analyzed during the current study are available from the corresponding author on reasonable request.

Code availability Not applicable.

Declarations

Ethics approval This research does not involve any human or animal participants. All professional ethics have been followed. The manuscript has not been submitted to other journals for simultaneous consideration.

Consent for publication All authors whose names appear on the submission have contributed sufficiently to the scientific work and therefore share collective responsibility and accountability for the results.

Competing interests The authors declare no competing interests.

References

1. Mirandola I, Quagliato L, Berti GA, Caracciolo R, Ryu SC, Perin M, Kim N (2022) Geometry evolution prediction and process settings influence in profiled ring rolling. Int J Adv Manuf Technol 122:799–819
2. Berti GA, Quagliato L, Monti M (2015) Set-up of radial–axial ring-rolling process: process work sheet and ring geometry expansion prediction. Int J Mech Sci 99:58–71
3. Wang ZW, Fan JP, Hu DP, Tang CY, Tsui CP (2010) Complete modeling and parameter optimization for virtual ring rolling. Int J Mech Sci 52:1325–1333
4. Cheng HQ, Bo JX, Qi HP, Fu JH, Li YT (2010) Establishment of hot processing maps and hot ring rolling process of 42CrMo steel. Mat Mech Eng 50:16–089
5. Qin FC, Qi HP, Li YT, Qi HQ (2020) Microstructure evolution in hot ring rolling of centrifugal casting Q235B steel. Mater Rep 34(12):12132–12138
6. Chang YD, Qi HP, Jia YL (2022) Experimental research on hot ring rolling of centrifugally cast bimetallic rings. Mater Rep 37:14–21110004
7. Sun ZC, Yang H, Xinzhe O (2010) Effects of process parameters on microstructural evolution during hot ring rolling of AISI 5140 steel. Comput Mater Sci 49:134–142
8. Ryttberg K, Wedel MK (2010) The effect of cold ring rolling on the evolution of microstructure and texture in 100Cr6 steel. Mater Sci Eng A 527(9):2431–2436
9. Wang M, Yang H, Zhang C, Guo LG (2013) Microstructure evolution modeling of titanium alloy large ring in hot ring rolling. Int J Adv Manuf Technol 66(9):1427–1437
10. Qian DS, Pan Y (2013) 3D coupled macro-microscopic FE modeling and simulation for combined blank-forging and rolling process of alloy steel. Comput Mater Sci 70:24–36
11. Tian X, Zhang H, Cheng F (2021) Macro-and microscopic simulation of ring rolling for aluminum alloy thin-walled special-shaped section ring. J Mech Eng 57(12):179–191
12. Qi SH, He F, Zhou YL (2022) Simulation research on effect of blooming temperature on radial-axial rolling forming of ring. J Plasticity Eng 29(3):79–86
13. Guo L, Pan X, Yang H, Liu X (2012) Multi-scale finite element simulation of microstructure response to rolling ratio for ring rolling process based on 42CrMo ingot blank. International conference on wind energy: Materials, engineering and policies, Hyderabad, India: NEI-DK-5854. https://www.osti.gov/etdeweb/biblio/22059274
14. Li J, Li YT, Qi HP, Chen HQ (2013) Effects of initial rolling temperature on rolling deformation and microstructure evolution of 42CrMo casting ring blank. Asme International Mechanical Engineering Congress & Exposition, San Diego, USA: IMECE2013-63055. https://doi.org/10.1115/IMECE2013-63055
15. Li YT, Li J, Qi HP, Zhang F (2014) Technology and experiments of 42CrMo bearing ring forming based on casting ring blank. Chinese J Mech Eng 27:418–427
16. Guo YN, Ding SF, Li YT, Qi HP, Qian DS, Guo LG (2014) Multiscale modeling for 42CrMo ring during blank-casting and rolling compound forming process. J Mech Eng 50(14):81–88
17. Mao HJ, Zhang R, Hua L, Yin F (2015) Study of static recrystallization behaviors of GCr15 steel under two-pass hot compression deformation. J Mater Eng Perform 24:930–935
18. Yin F, Hua L, Mao HJ, Han XH (2013) Constitutive modeling for flow behavior of GCr15 steel under hot compression experiments. Mater Des 43:393–401
19. Yin F, Hua L, Mao HJ, Han XH, Qian DS, Zhang R (2014) Microstructural modeling and simulation for GCr15 steel during elevated temperature deformation. Mater Design 55:560–573
20. Hua L, Huang XG, Zhu CD (2001) Theory and technology of ring rolling. China Machine Press (in Chinese)
21. Sun ZC, Yang H, Ou XZ (2008) Thermo-mechanical coupled analysis of hot ring rolling process. Trans Nonferrous Metals Soc China 18(5):1216–1222
22. Guo J, Qian DS, Deng JD (2016) Grain refinement limit during hot radial ring rolling of as-cast GCr15 steel. J Mater Proc Technol 231:151–161